Available online at www.sciencedirect.com

SciVerse ScienceDirect

Procedia Engineering 47 (2012) 1025 – 1028

Procedia Engineering

www.elsevier.com/locate/procedia

Proc. Eurosensors XXVI, September 9-12, 2012, Kraków, Poland

Electrical impedance detection of senescence in adipose tissue-derived stem cells

Hee-Sook Jun[a,b], Lan Thi Mai Dao[b], Sungbo Cho[c] *

[a]*College of Pharmacy, Gachon University, 191 Hambakmoe-ro Yeonsu-gu, Incheon, 406-799, Korea*
[b]*Lee Gil Ya Cancer and Diabetes Institute, Gachon University, 7-45 Songdo-dong Yeonsu-gu, Incheon, 406-840, Korea*
[c]*Department of Biomedical Engineering, Gachon University, 191 Hambakmoe-ro Yeonsu-gu, Incheon, 406-799, Korea*

Abstract

For stem cell-based tissue engineering or tissue therapy, control of the quality of isolated stem cells is required. In this study, we used the electrical impedance spectroscopy to characterize the effect of passage on the morphological change and the proliferative capacity of adipose tissue-derived stem cells (ADSCs) during cell growth on the transparent ITO electrodes. ADSCs adhered to the ITO electrode and proliferated during cell growth. The phase contrast image of ADSCs on the electrode showed that the cells at passage 9 had a small and spindle-shaped morphology while the cells at passage 31 were flattened and larger than younger cells. The real part of the impedances of passage 9 cells were lower than passage 31 at the beginning time of culture due to the larger size of older cells adhered to the electrode. Then, the values of passage 9 cells were increased and distinguishable from passage 31 due the higher proliferation rate of younger cells. The experimental results showed that the impedance measurement could characterize the age-related morphological change and the proliferative capacity of ADSCs during cell growth.

Keywords: Aging; Cell morphology; Impedance spectroscopy; Stem cells; ITO electrode

1. Introduction

New treatment strategies based on stem cell tissue engineering or therapy take advantage of the long-term self-renewal capacity and multi-lineage differentiation potential that stem cells offer. Human mesenchymal stem cells can be isolated from bone marrow and differentiated into a specific type of tissue cell in vitro, which can then be used as a source of cells for transplantation. Adipose tissue or umbilical

* Corresponding author. Tel.: +82-32-820-4433; fax: +82-32-820-4059.
E-mail address: sbcho@gachon.ac.kr.

doi:10.1016/j.proeng.2012.09.323

cord blood are also sources of stem cells, however isolation of stem cells from bone marrow is a highly invasive procedure [1]. Because the proliferative capacity and multipotency of stem cells is dependent on the type and age of the source tissue, a standardized method during cell isolation and quality control measures are required. To assure cell quality it is preferable to use non-invasive, real-time monitoring methods instead of label-based assays, the latter of which can alter cell properties.

A non-invasive, real-time method for characterizing cells is to measure the electrical impedance of cells cultured on electrodes. Using electrical impedance measurements, it was able to characterize the toxic effect of chlorpyrifos on stem cells undergoing adipogenic differentiation [2] or to monitor the impedance change in stems during differentiation into osteoblasts [3]. However, the impedance measurement of stem cells was not yet applied to characterize cell senescence although age-related growth rate and viability determine their differentiation properties. In this study, it was investigated whether the impedance of adipose tissue-derived stem cells (ADSCs) is affected by the cell passage number, and whether the measured data reflect the cell morphology and proliferative capacity of cells at different passage number. For the optical and electrical characterization of cells, the indium tin oxide (ITO) electrode-based cell chip which provides better transparency than gold or platinum was applied.

2. Methodology

2.1. Fabrication of ITO Electrode-based Chip

Glass slides coated by ITO and with a sheet resistance of 4 Ω/sq were purchased (Taeyoung Optics, Incheon, Korea). The conductive ITO layer was ablated to pattern working and counter electrodes with their corresponding transmission lines and terminal pads by laser processing (μ-Fab, KORTherm Science, Incheon, Korea). Parylene-C, which meets U.S. Pharmacopoeia Class VI biocompatibility requirement, was deposited onto the patterned ITO substrate by chemical vapor deposition (PDS 2010, Specialty Coating System Inc., Indianapolis IN, USA). The deposition rate and thickness of parylene-C were 14 nm/min and 550 nm, respectively. After deposition, the surfaces of the working electrode, counter electrode and terminal pad sites were exposed by photolithography and reactive ion etching (ADE-4600, A-Tech System, Incheon, Korea). The final working electrode area was circular with a diameter of 400 μm, and the working electrodes were separated by more than 2 mm from the relatively large counter electrode.

2.2. Electrical Impedance Measurement

After a polystyrene chamber was bound to the electrode substrate using an adhesive silicone rubber, 1 x 10^3 of ADSCs and 800 μl of culture medium were placed in the chamber. The electrode chip was mounted in a homemade electrical adapter connecting the terminal pads of the electrode substrate with a digital lock-in-amplifier (SR830, Stanford Research Systems, Sunnyvale CA, USA). The amplitude of the input current was restricted to 100 nA by serially connecting a 100 kΩ resistor to the internal function generator of the lock-in-amplifier, which resulted in the maximum current density at the working electrode below 79.6 μA/cm^2. The electrical impedance value was ascertained by calculating the ratio of the measured in-phase and out-of-phase potential response to the applied input current, in the 100 Hz to 100 kHz frequency range. The equivalent circuit model for the total impedance spectrum of the cell-covered electrode was designed as the sum of a constant phase element for the interfacial electrode impedance (CPE_{el}), the cell impedance modelled using a cell layer resistance (R_{cl}) in parallel with a cell layer capacitance (C_{cl}), and the resistance of the medium (R_m) [4].

3. Results and Discussion

ADSCs adhered to the ITO electrodes and proliferated, with the resulting morphology and growth behaviour comparable to those on a standard culture dish. Fig. 1 shows phase contrast images of the ADSCs on the ITO working electrode at passage 31. ADSCs at passage 9 had a small, spindle-shaped morphology, but the cells at passage 31 were larger and flattened, an indication of expected cell morphology changes that accompany passage. While the number of ADSCs on the circular exposed area of the working electrode at passage 9 increased rapidly, the increase of cell number in passage 31 cells was considerably slower.

Fig. 2 shows the real and imaginary parts of the impedance with or without ADSCs at passage 9 measured at 304 h of incubation time (marked points), together with the fitted lines using the equivalent circuit of [4. The values of R_{cl} and C_{cl} extrapolated by curve fitting were 3210 Ω and 1.26 nF, when CPE_{el} and R_m were 4.28 x 10^7 / $(i\omega)^{0.92}$ Ω and 978 Ω, respectively. The measured impedance spectrum of the bare ITO electrode without cells was characterized by CPE_{el} and the series R_m. In the case of the cell-covered electrode impedance spectrum, the real part of the impedance increased in the intermediate frequency range as compared to the electrode without cells, whereas the imaginary part of the impedance was higher than the value without cells at frequencies above 10 kHz due to the dielectric property of the cell membrane.

Fig. 3a shows the ratio of the resistance of the ITO electrode with ADSCs at passage 9 as compared to the bare electrode without cells (normalized real part of the impedance). The normalized value increased with culture time, and the degree of normalized value increase was dependent on frequency. The greatest change in normalized value during cell growth was observed between 1 and 5 kHz. Fig. 3b illustrates the average and standard deviation of the normalized value at 2.15 kHz measured with ADSCs at passage 9 or 31 (n = 4/group). The values of passage 31 cells were higher than passage 9 at the beginning of culture due to the larger size of older cells adhered to the electrode. Then, the values of passage 9 cells were increased and distinguishable from passage 31 due the higher proliferation rate of younger cells. Thus, the age-related morphological change and proliferative capacity of ADSCs can be characterized.

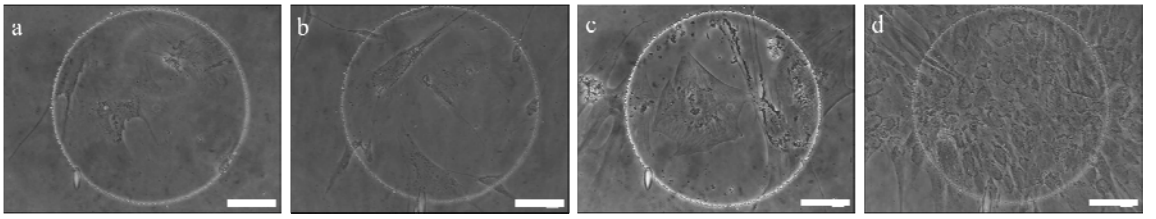

Fig. 1. ADSCs at passage 31 (a, c) or passage 9 (b, d) on the circular ITO electrode after 100 h (a, b) or 300h (c, d) of incubation, scale bar: 80 μm.

Acknowledgements

This research was supported by Basic Science Research Program through the National Research Foundation of Korea (NRF) funded by the Korean Ministry of Education, Science and Technology (No. 2011-0026948), and by a grant from Innovative Research Institute for Cell Therapy Project, Korean Ministry for Health, Welfare & Family Affairs, Republic of Korea (A062260).

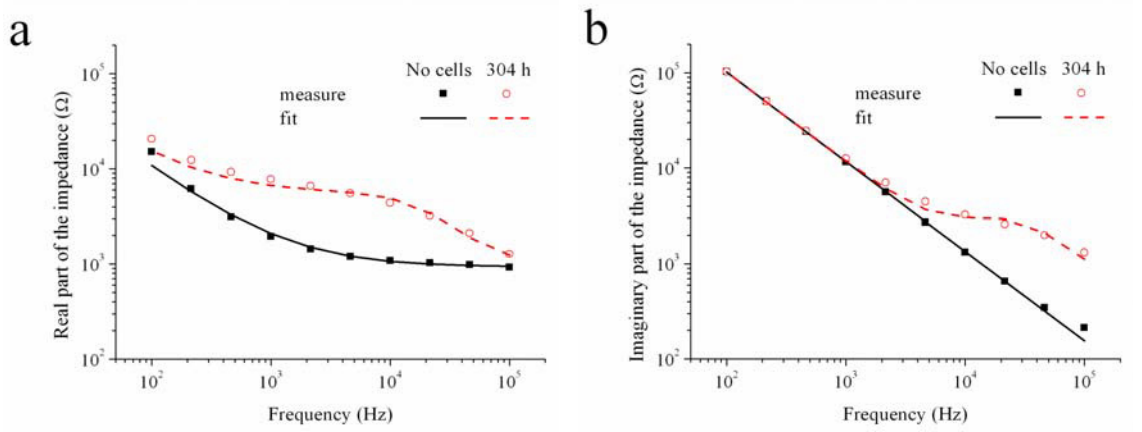

Fig. 2. (a) Real and (b) imaginary parts of the impedance of the ITO electrode, together with the fitted lines using an equivalent circuit model, the sum of a constant phase element for the interfacial electrode impedance, the cell impedance modelled using a resistance in parallel with a capacitance, and the medium resistance (fit), with or without ADSCs at passage 9 (304 h of incubation), and frequency range of 100 Hz to 100 kHz (measure).

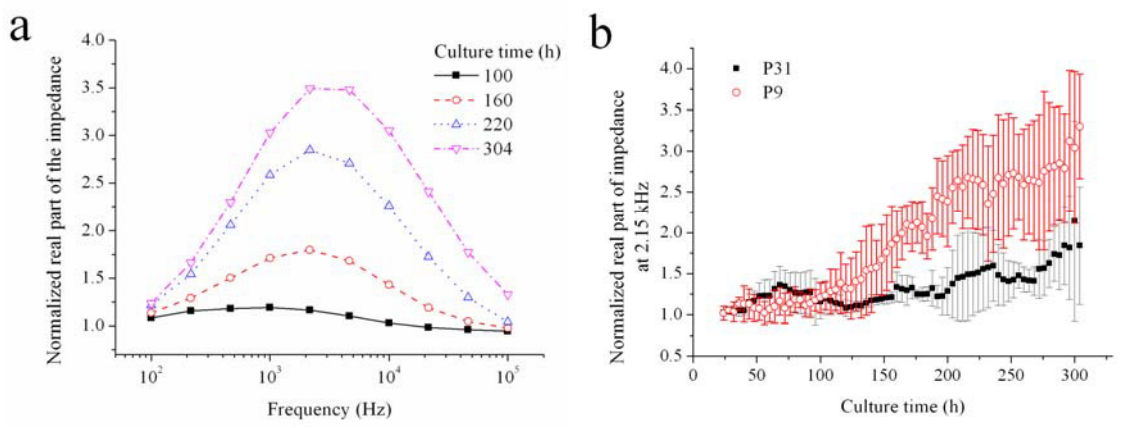

Fig. 3. (a) Ratio of the resistance of the ITO electrode with ADSCs at passage 9, to the resistance of the bare electrode without cells (normalized real part of the impedance), measured at 100 h, 160 h, 220 h or 304 h of incubation time, and (b) normalized real part of impedance at 2.15 kHz and passage 31(P31) or 9 (P9). Data shown to include mean ± SD (n = 4/group).

References

[1] Kern S, Eichler H, Stoeve J, Klüterand H, Bieback K, Comparative analysis of mesenchymal stem cells from bone marrow, umbilical cord blood, or adipose tissue. *Stem Cells* 2006;**24**:1294–301.

[2] Cho S, Gorjup E, Thielecke H, Chip-based time-continuous monitoring of toxic effects on stem cell differentiation. *Annals of Anatomy* 2009;**191**:145-52.

[3] Hildebrandt C, Büth H, Cho S, Impidjati, Thielecke H, Detection of the osteogenic differentiation of mesenchymal stem cells in 2D and 3D cultures by electrochemical impedance spectroscopy. *Journal of Biotechnology* 2010;**148**:83-90.

[4] Wegener J, Zink S, Rösen P, Galla HJ, Use of electrochemical impedance measurements to monitor β-adrenergic stimulation of bovine aortic endothelial cells. *Pflugers Arch* 1999;**437**:925-34.